The Impact of Graph Construction Scheme and Community Detection Algorithm on the Reliability of Community and Hub Identification in Structural Brain Networks

Stavros I. Dimitriadis[1-6,8*], Eirini Messaritaki[1,2,3,7], Derek K. Jones[1,3,8]

1. Cardiff University Brain Research Imaging Centre (CUBRIC), School of Psychology, Cardiff University, Maindy Road, Cardiff, CF24 4HQ, UK
2. Division of Psychological Medicine and Clinical Neurosciences, School of Medicine, Cardiff University, Cardiff, CF24 4HQ, UK
3. School of Psychology, Cardiff University, 70 Park Place, Cardiff, CF10 3AT, UK
4. Neuroinformatics Group, Cardiff University Brain Research Imaging Centre, School of Psychology, Cardiff University, Cardiff, United Kingdom
5. Neuroscience and Mental Health Research Institute, Cardiff University, Cardiff, United Kingdom
6. MRC Centre for Neuropsychiatric Genetics and Genomics, School of Medicine, Cardiff University, Cardiff, United Kingdom
7. BRAIN Biomedical Research Unit, Cardiff University, Maindy Road, Cardiff, CF24 4HQ, UK
8. Mary McKillop Institute for Health Research, Faculty of Health Sciences, Australian Catholic University, Melbourne, Australia

*Corresponding author:
Stavros I. Dimitriadis
Contact:DimitriadisS@cardiff.ac.uk / stidimitriadis@gmail.com
Cardiff University Brain Research Imaging Centre (CUBRIC), School of Psychology, Cardiff University, Maindy Road, Cardiff, CF24 4HQ, UK

Abstract:

The human brain is a complex network of volumes of tissue (nodes) that are interconnected by white matter tracts (edges). It can be represented as a graph to allow us to use graph theory to gain insight into normal human development and brain disorders. Most graph theoretical metrics measure either whole-network (global) or node-specific (local) properties of the network. However, a critical question in network neuroscience is how nodes cluster together to form communities, each of which possibly plays a specific functional role. Community partition analysis allows us to investigate the mesoscale organization of the brain. Various algorithms have been proposed in the literature, that allow the identification of such communities, with each algorithm resulting in different communities for the network. Those communities also depend on the method used to weigh the edges of the graphs representing the brain networks. In this work, we use the test-retest data from the Human Connectome Project to compare 32 such community detection algorithms, each paired with 7 graph construction schemes, and assess the reproducibility of the resulting community partitions.

The reproducibility of community partition depended heavily on both the graph construction scheme and the community detection algorithm. Hard community detection algorithms, via which each node is assigned to only one community, outperformed soft ones, via which each node can be a part of more than one community. The best reproducibility was observed for the graph construction scheme that combines 9 white matter tract metrics paired with the greedy stability optimization algorithm, with either discrete or continuous Markovian chain. This graph-construction scheme / community detection algorithm pair also gave the highest similarity between representative group community affiliation and individual community affiliation. Connector hubs were better reproduced than provincial hubs.

Keywords: Structural Brain network, Community detection, “Ground truth”, Permutation test, Normalized Mutual Information (NMI), Diffusion Magnetic Resonance Imaging (dMRI), hard community detection, soft community detection, overlapping communities.

1. Introduction

The human brain can be modelled as a network, both from a structural and a functional perspective (Bassett and Sporns, 2017) and summarised as a graph. The nodes of the graph are small volumes of tissue which are interconnected via white matter tracts for structural networks, or which exhibit correlations of functional activity for functional networks (Avena-Koenigsberger et al., 2017). The connections between nodes are also called edges. Graph theory can provide novel insights into healthy human brain function (Bassett et al., 2011; Braun et al., 2015) and its alteration in various diseases (Braun et al., 2016, Baker et al. (2015); Collin et al. (2016); Drakesmith et al. (2015); Aerts et al. (2016); Nelson et al. (2017); Vidaurre et al. (2018); Imms et al. (2019)). An open question in network neuroscience is how neural units cluster together to form inter-connected groups and to provide the coordinated brain activity that gives rise to action, perception and behaviour (Bassett and Mattar, 2017; Pessoa et al., 2018).

Commonly-studied graph theoretical measures include global and local efficiency, clustering coefficient, shortest path length, small-worldness, etc (Rubinov and Sporns 2010). However, although these metrics can provide useful information related to the global and local properties of the network, it is community (or modularity) detection techniques, that are more appropriate to investigate the *mesoscale* network organization (Meunier et al. 2010). Modularity is a quintessential concept in network neuroscience, wherein neural units are densely connected to one another, forming clusters or *modules* (Meunier et al., 2010). Modular organization is an efficient architecture that allows a complex network to integrate information locally, while maintaining its adaptability to any external stimulus. Community structure analysis is one of the most important fields in complex networks, as networks in nature often show hierarchical, modular organization (Blondel et al., 2008; Fortunato 2010; Fortunato and Castellano 2012; A. Lancichinetti and Fortunato 2009a,b; Newman,2004 2012; Meunier et al., 2009). In the brain, such hierarchical modularity could support segregated neuronal interactions and their integration at the global level. Networks with such structure (Fortunato, 2010) are more complex than those with random structure (Sporns et al., 2000), and have been well demonstrated in functional brain networks (Sporns and Betzel, 2016).

The main core of network metrics measure global and local properties like degree, shortest path length etc. derived from network topology and characterizing networks at the extreme topological scales: at the scale of the network's individual nodes or at the scale of the whole

network (Giusti et al., 2016). However, neither extreme topological scales inform us about the *intermediate* scale at which a network can be characterized.

Various methodologies for structural network generation have been proposed, involving tractography with different algorithms and assigning edge weights using different diffusion MRI-based metrics. The resulting graphs are quite different from each other, and have different levels of robustness and reproducibility (Messaritaki et al., 2019a). Several research articles have investigated different aspects of the reproducibility of structural brain networks and the related network metrics (Smith et al., 2015; Owen et al., 2013, 2013; Zhong et al., 2015; Dimitriadis et al., 2017b; Yuan et al., 2019), each using a different graph construction scheme and predominantly using data acquired with low diffusion weightings (*b*-values of up to 1500 s/mm^2). We recently explored the reproducibility of structural brain graphs, their edge weights and graph-theoretical metrics, for 21 different edge-weighting schemes (Messaritaki et al., 2019a).

A frequently-used methodology to identify/classify the community structure of networks is based on two modular network metrics: the participation coefficient, P_i; and the within-module z-score, z_i. Both metrics require the detection of community partitions of the brain network (Guimera et al., 2005; van den Heuvel and Sporns, 2013). The P_i of a node quantifies the distribution of its links among the modules of the network, while z_i measures the connectedness of a node to other nodes in the module. See Appendix 1 for more detail.

In this work, we constructed structural brain networks from a set of repeat diffusion MRI scan data from the Human Connectome project using the b=2000 s/mm^2 data and the seven most reproducible graph-construction schemes as derived from our previous study on the same dataset (Messaritaki et al., 2019b). We then estimated the reproducibility of nodal P_i and z_i and also the detection of provincial and connector hubs, based on both modular network metrics. Our aim was to identify the optimal combination of graph construction scheme and community detection algorithm from the perspective of reproducibility. The reproducibility criterion was the highest agreement of individual communities between two repeat scan sessions. Finally, we derived a consensus cluster across subjects and repeat scans (Dong et al., 2014; Ozdemir et al., 2015). The agreement of consensus cluster with individual communities was also used as an objective criterion of the best combination of graph construction scheme and community detection algorithm. The reason we look into the reproducibility of the community partitions is that the results of a robust brain network analysis must be reproducible, within experimental error, when generated from data collected at different times, in the absence of any true changes in the structural connectome. Community partitions that are not reproducible in the absence of

age-related changes or intervention-induced plasticity are not reliable representations of the mesoscale organization of the human brain.

The rest of this manuscript is organised as follows: Section 2 describes the graph-construction schemes, community detection algorithms, community partition similarity, the methodology of the detection of connector and provincial hubs and their reproducibility. Section 3 reports our results in terms of reproducible community partitions across the 2D space of graph-construction schemes / community detection algorithms, the reproducibility of nodal P_i/ z_i and the detection of connector/provincial hubs. The Discussion section describes the main outcome of our study explaining its advantages, limitations, suggestions for researchers and future directions.

2. Methods

2.1. Data

We analysed the test-retest MRI and diffusion-MRI dataset from the multimodal neuroimaging database of the Human Connectome Project (HCP) (Sotiropoulos et al., 2013b; Glasser et al., 2013). Thirty-seven participants on this test-retest dataset were scanned twice with the between-scan time interval ranging between 1.5 and 11 months, while the age range of the participants was 22–41 years. The test-retest time interval is shorter than the expected time over which maturation-induced structural changes can be measured with diffusion MRI (dMRI).

The diffusion-weighted images (DWIs) have resolution of (1.25×1.25×1.25) mm^3 and were acquired for three different diffusion weightings (*b*-values: 1000 s/mm^2, 2000 s/mm^2 and 3000 s/mm^2) across 90 gradient directions for each *b*-value. The HCP acquisition details are described in Sotiropoulos et al. (2013a,b). We performed the analyses described in the following sections using the dataset acquired with b=2000 s/mm^2.

2.2. Tractography

We performed whole-brain tractography using ExploreDTI-4.8.6 (Leemans et al., 2009). Constrained Spherical Deconvolution (CSD) (Tournier et al., 2004) was used to estimate the fiber orientation distribution function (fODF). In the tractography algorithm, the seed point resolution was $(2\times2\times2\ mm)^3$, the step size was 1 mm, the angular threshold was 30°, and the fiber length range was 50−500 mm.

2.3. Graph generation

2.3.1. Node definition

We employed the Automated Anatomical Labeling (AAL) atlas (Tzourio-Mazoyer et al., 2002) to define the 90 cortical and subcortical areas of the cerebrum (45 areas per hemisphere) that define the nodes of the structural brain graphs. These nodes are connected via white matter (WM) tracts, which are the edges or connections of the brain network. The network generation was performed in ExploreDTI-4.8.6 (Leemans et al., 2009) and generated structural brain networks (SBN) for each participant.

2.3.2. Edge weights

We weighted each edge using the seven most reproducible (out of 21) different graph-construction schemes as they were explored in our previous analysis on the same dataset (Messaritaki et al., 2019b). Those seven graph construction schemes (see Section 2.3.4) were based on different combinations of the following metrics: fractional anisotropy (FA), mean diffusivity (MD), radial diffusivity (RD), number of streamlines (NS), streamline density (SLD), percentage of streamlines (PS), tract volume (TV), tract length (TL) and Euclidean distance between the nodes (ED) (see Table 1). We normalized all graphs so that the maximum edge weight in each graph was equal to 1 while the elements in the main diagonal were set to zero (see Figure 1).

Table 1. Metrics used in connectivity matrices.

Metric	Abbreviation
Fractional anisotropy	FA
Mean diffusivity	MD
Radial diffusivity	RD
Number of streamlines	NS
Percentage of streamlines	PS
Streamline density	SLD
Tract volume	TV
Tract length	TL
Euclidean distance between nodes	ED

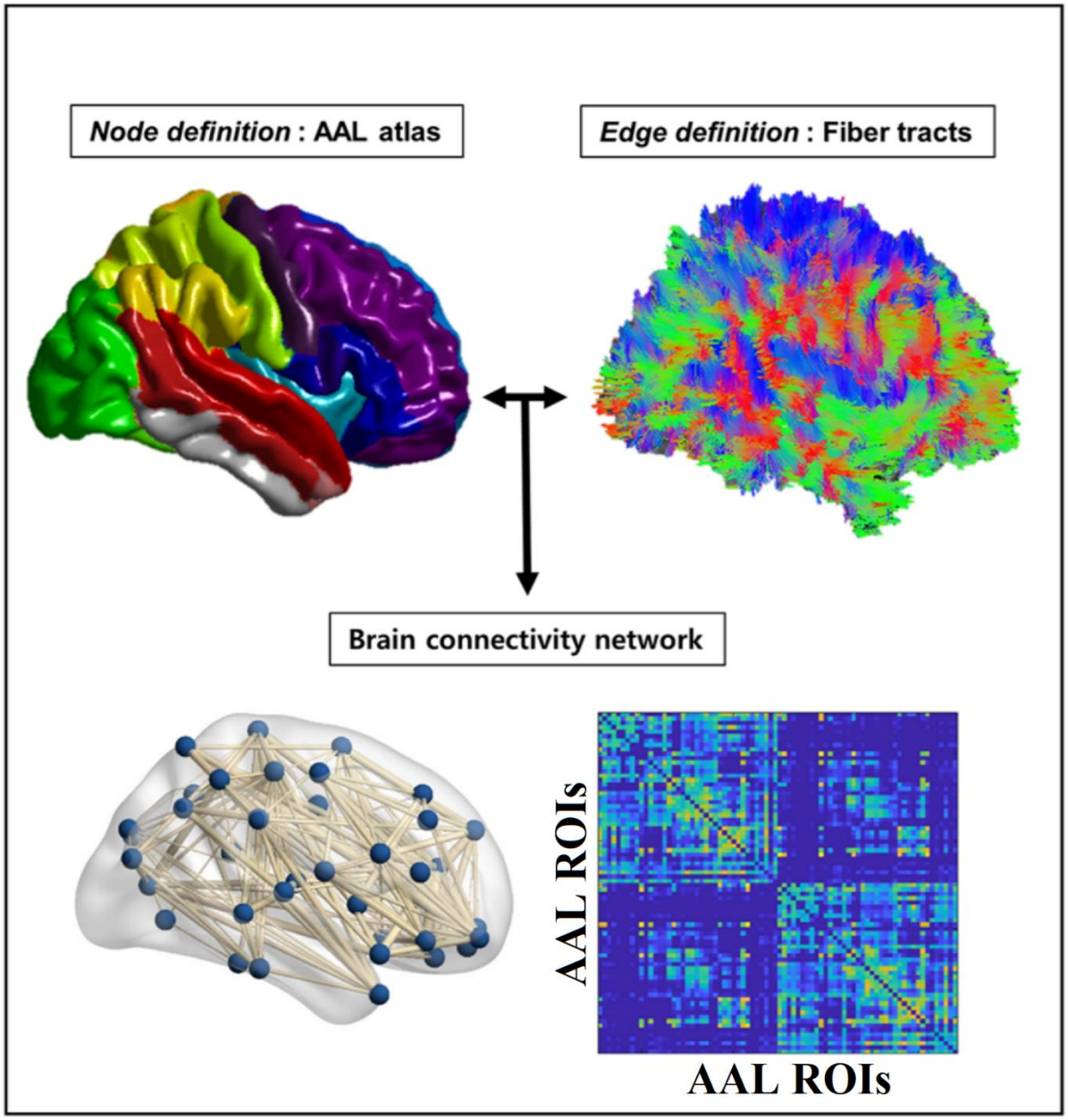

Figure 1. Flowchart of the construction of a structural brain network based on tractography and diffusion metrics (see Table 1).

2.3.3 Integrated Structural Brain Graphs

Combining different metrics of the white matter tracts into an *integrated* edge weight is supported by the fact that each one measures complementary information, while topological properties of SBNs are affected by more than one. In two previous works, Nigro et al., (2016) employed the product of NS and FA to weight the SBNs of Parkinson's patients, while Taylor

et al. (2015) used a combination of NS and TL for constructing SBNs for epilepsy patients. In the current work, the integration of the nine individual metrics has been realized with the data-driven algorithm described in our previous work (Dimitriadis et al., 2017b,c), resulting in an integrated SBN for each participant and scan session. Details of the algorithm and its implementation can be found in our previous work (Dimitriadis et al., 2017a,b,c; Messaritaki et al., 2019). The main feature of the algorithm is that it maximises the information included in all the metrics used, rather than relying exclusively in any one of them.

2.3.4 Graph Construction Schemes

A total of seven graph construction schemes were used in this study, falling into two broad approaches.

In the first approach, graphs were constructed by: (1) applying the orthogonal minimal spanning tree filtering algorithm (OMST, Dimitriadis et al., 2017b,c) directly to the NS edge-weighted matrix; (2) integrating the NS-weighted and FA-weighted matrices with the data-driven algorithm; and (3) integrating all nine diffusion metrics as originally reported in Dimitriadis et al. (2017b, see Table 2).

In the second approach, we constructed SBNs with edges weighted by the NS and FA and applying a threshold to remove edges with the lowest weights. Rather than imposing an arbitrary threshold, an absolute threshold was determined by imposing the constraint that the graphs exhibit the same sparsity as the OMST graphs that exhibited the highest reproducibility (Messaritaki et al., 2019b). Once the topology of each of those graphs was specified, the weights of the edges were either kept as they were or re-weighted with one of the remaining two metrics. As a result, the second set of graph-construction schemes that we studied here was: 4) keeping the highest-NS edges; 5) keeping the highest NS edges and reweighting with FA; 6) keeping the highest NS edges and reweighting with MD; and 7) keeping the highest FA edges and reweighting with NS .

Table 2. Summary of the graph-construction schemes

Abbreviation	Initial Edge Weights	Topology	Final Edge Weights
NS – OMST	NS	OMST	Unchanged
NS + FA OMST	lin. comb. of NS and FA	OMST	Unchanged
9-m OMST	lin. comb. of all 9 metrics in Table 1	OMST	Unchanged
NS-thr	NS	keep highest-NS edges	Unchanged
NS-t/FA-w	NS	keep highest-NS edges	re-weight with FA
NS-t/MD-w	NS	keep highest-NS edges	re-weight with MD
FA-t/NS-w	FA	keep highest-FA edges	re-weight with NS

2.3.5 Community detection algorithms

Communities or modules are defined as subgroups of nodes in a network that are more interconnected between each other compared to the rest of the network (Newman and Girvan 2004; Radicchi et al. 2004). While the list of community detection algorithms is large, they can be broadly classified into hard and soft clustering approaches. In the present study, we compared thirty-two different community detection algorithms, comprising twenty five with hard clustering and six with soft clustering. Figure 2 demonstrates the difference between hard and soft clustering. In hard clustering, community membership can be represented as a vector that encapsulates the assignments of every brain area to every detected graph cluster (community). In our case, clustering has a dimension of 1 x 90, equalling the number of brain regions in the AAL parcellation. In soft clustering, the outcome is a matrix that encapsulates how many soft clusters a given brain area belongs to.

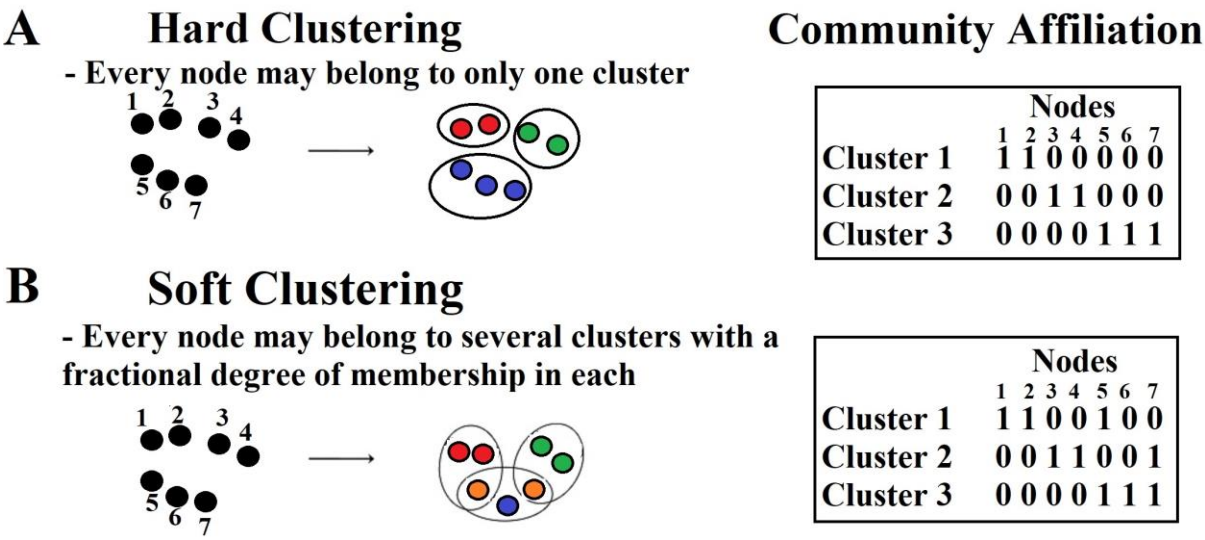

Figure 2. **An example of hard and soft clustering in a toy example containing 7 nodes.**

A. Hard clustering: A node can only belong to one cluster. The table tabulates the community assignment to every node.

B. Soft clustering: Five out of seven nodes are clustered in a single cluster/community {nodes 1,2,3,4,6} while nodes {5 and 7} belong to two communities : node 5 belongs to communities 1 and 3 while node 7 belongs to communities 2 and 3. The table tabulates the community assignment to every node.

Hard clustering algorithms are divided into three groups:

A. Fast multi-scale community detection algorithms:

1. (fast_mo): Fast greedy modularity optimisation algorithm based on the multi-scale algorithm but optimised for modularity (mono-scale) (Le Martelot and Hankin, 2012a,b).
2. (mscd_afg): Fast multi-scale community detection algorithm using the criterion from Arenas et al. (2008)
3. (mscd_hslsw): Fast multi-scale community detection algorithm using the criterion from Huang et al. (2011)
4. (mscd_lfk): Fast multi-scale community detection algorithm using the criterion from Lancichinetti et al. (2009b)
5. (mscd_rb): Fast multi-scale community detection algorithm using the criterion from Reichardt & Bornholdt, (2006)

6. (mscd_rn): Fast multi-scale community detection algorithm using the criterion from Ronhovde & Nussinov (2009)
7. (mscd_so): Fast multi-scale community detection algorithm using stability optimisation (Le Martelot and Hankin, 2012).

B. **Multi-Scale Community Detection algorithms using Stability as Optimisation Criterion in a Greedy Algorithm and Multi-Scale Community Detection using Stability Optimisation as described in (Le Martelot and Hankin,2011):**

8. (gso_discrete): Greedy stability optimisation using the Markov chain model.
9. (gso_continuous): Greedy stability optimisation using a time-continuous Markov process.
10. (msgso_discrete): Multi-step greedy stability optimisation using the Markov chain model.
11. (msgso_continuous): Multi-step greedy stability optimisation using a time-continuous Markov process.
12. (rgso_discrete): Randomised greedy stability optimisation using the Markov chain model.
13. (rgso_continuous): Randomised greedy stability optimisation using a time-continuous Markov process.
14. (gso_discrete_markovian): Front-end function calling any of the aforementioned algorithms based on discrete Markovian model. We specified a pre-processing phase removing nodes with a single neighbour and a post-processing phased based on the Kernighan-Lin algorithm adapted for stability (Kernighan and Lin,1970).
15. (gso_discrete_continuous): Same as above but based on continuous Markovian model.
16. (Newman): Greedy modularity optimisation with Newman's fast algorithm.
17. (Danon): Greedy optimisation of Danon et al.'s criterion (Danon et al., 2006).
18. (Louvain): Uses the Louvain method (Blondel et al.,2008)
19. (Louvain_modularity): Uses the Louvain method to optimise modularity criterion with gamma=0.5.
20. (**Louvain_so**): Uses the Louvain method to optimise ‘stability’ criterion with Markovian time
21. (reichardt): Greedy optimisation of Reichardt & Bornholdt's criterion (Reichardt and BornHoldt, 2006).

22. (ronhovde): Greedy optimisation of Ronhovde & Nussinov's criterion (Reichardt and BornHoldt, 2006)

C. Hard community detection algorithms involving a set of state of the art graph partition algorithms (three of them have been designed for, and applied in, computer vision).

23. (shi_malik): From tens of available spectral clustering algorithms, we adopted the most famous representative algorithm from Shi and Malik, (2000)
24. (dominant_sets): Dominant sets (Pavan and Pelillo, 2007). We have adopted this algorithm in our previous studies (Dimitriadis et al., 2009,2012)
25. (modularity): The famous Modularity algorithm (Newman, 2006)
26. (infomap): Infomap proved an important algorithm for identifying communities in large graph-oriented problems and synthetic graphs (Rosvall M, Bergstrom CT, 2008))

The soft clustering algorithms we considered are:

27. (ogso_discrete): Greedy stabilisation optimisation with overlapping communities for discrete Markov Model. The network is first converted to an edge-graph and then community detection is performed on the edge-graph
28. (ogso_continuous): Greedy stabilisation optimisation with overlapping communities for continuous Markov Model. The network is first converted to an edge-graph and then community detection is performed on the edge-graph
29. (link): Link Communities: The network is first converted to an edge-graph and then community detection is performed on the edge-graph. In an edge-graph, nodes refer to edges of the original SBN while edges denote edges between pair of connected edges of the original SBN. This algorithm uncovers overlapping community structure via hierarchical clustering of network links (Ahn et al., 2010). We used single-linkage criterion.
30. (link_complete): Link Communities: Same as above but we used complete-linkage criterion.
31. (nnmf): Non-negative Matrix Factorization (NNMF): (Psorakis et al., 2011)
32. (k-cliques): This algorithm partitions a graph into soft communities using the simplest subgraph forms, the k-cliques. Here, we used 3-cliques (Palla et al., 2005)

For the first set of multiscale community detection algorithms, we considered the following set of resolution parameter ps=[0.1 0.15 ,…,0.55,0.60]. For the discrete and continuous Markovian time series, we searched over ts=[0.1,0.02,…,0.9,1.0] . Finally, for Louvain's modularity method and Reichardt's method, we considered γ = [0.05,0.1,0.15,…,0.95,1.0]. The aforementioned parameters were optimized over the highest group-averaged community affiliation similarity between the two scans estimated with NMI. For further details, see the following section.

For the Louvain's methods, we ran the algorithms 1000 times and we followed the construction of consensus matrix approach. We represented this approach in section 2.3.8 for the construction of consensus matrix across subjects and scans.

2.3.6 Permutation Test on Quality Modular Indexes

All the aforementioned methods, with the exception of no. 29-32 of the soft clustering algorithms, involve a Q quality index for the hard or soft communities detected. For further details of Q quality indexes see **Le Martelot and Hankin,2011,2012a,b.** For that purpose, and to avoid the inflation of statistical noise of many techniques potentially trapped in local maxima, we followed a surrogate null-model approach. We produced 1000 surrogate null models for every SBN independently for every subject, scan and graph construction method by randomizing the weighed connections while preserving both the degree and strength of every node and the overall connectedness of the network (Rubinov and Sporns,2010). For soft clustering algorithms no. 29-32, we estimated the NMI between the original community affiliation and the surrogate null communities produced via the application of every algorithm to the surrogate graph model.

2.3.7 Between-Scan Community Detection Agreement

To assess the reproducibility of the thirty-two community detection techniques across the seven graph-construction schemes and repeat-scan sessions, we first quantified the similarity between the community partitions from the two scan sessions separately for every participant. For that purpose, we adopted the Normalized Mutual Information (NMI) (Alexander-Bloch et al. 2012), which is one of the most popular similarity measures based on information theory.

NMI is defined as follows (Lancichinetti and Fortunato,2009a):

$$NMI(A,B) = \frac{-2\sum_{i=1}^{C_A}\sum_{j=1}^{C_B} N_{ij}\log\left(\frac{N_{ij}N}{N_{i.}N_{.j}}\right)}{\sum_{i=1}^{C_A} N_{i.}\log\left(\frac{N_{i.}}{N}\right) + \sum_{j=1}^{C_B} N_{.j}\log\left(\frac{N_{.j}}{N}\right)} \quad (1)$$

where A and B are the community partitions of two SBNs from the two scan sessions while C_A , C_B are the number of communities in partition A and B, correspondingly. N defines the number of nodes (here 90), while N_{ij} is the overlap between A's and B's communities i and j which practically means the number of common nodes between the two partitions. N_i and N_j are the total number of nodes in A's and B's communities i and j, correspondingly. The NMI ranges from 0 to 1 where 0 corresponds to two independent partitions and 1 to identical partitions. This definition was used for hard community partition comparisons while for soft community partition (i.e. those with nodes in more than one communities) we adopted the homologue definition of NMI tailored to soft graph clustering (Lancichinetti et al., 2009a).

We estimated NMI values between every possible pair of scans and for each of the seven graph-construction schemes and the thirty-two community detection algorithms giving an exploratory space of {7 graph-construction schemes x 32 community detection algorithms}. The NMI was then averaged across the 37 participants, to create a group-averaged NMI. Below, we summarize the evaluation of the best community detection algorithm. We ranked the thirty-two community detection algorithms that demonstrated high test-retest reproducibility (group-averaged values NMI > 0.9) in at least one of the seven graph construction schemes (see Figure 4).

2.3.8 Consensus Clustering

For every graph construction scheme, a consensus matrix was constructed by integrating the community partitions across the highly reproducible community detection algorithms (group averaged NMI > 0.9).

A consensus matrix was constructed for every pair of {graph construction scheme – community detection technique} that showed high test-retest reproducibility across the cohort (group-averaged NMI > 0.9). We quantify how many times two nodes across the 74 SBNs (37 participants x 2 scans) are classified on the same community and this entry $t_{i,j}$ is assigned to the relevant pair of nodes. The consensus matrix has size equal to the original SBN and in our case

is a 2D matrix of size 90 x 90 with entries weighted from 0 up to 74 {37 subjects x 2 number of scans} in the optimal scenario. Entries of the consensus matrix were transformed to probabilities to denote the probability of occurrence of a pair of nodes (brain areas) being classified as belonging to the same community across the cohort and scan sessions.

In order to get a consensus or group representative community per case, consensus matrices should be iteratively thresholded and clustered with a community detection algorithm (Lancichinetti and Fortunato, 2012). This algorithm uses an absolute arbitrary threshold to eliminate weak connections and iteratively apply a graph partition technique. Instead of an arbitrary filtering scheme, we adopted our OMST algorithm (Dimitriadis et al., 2017a,b,c) to topologically-filter the consensus matrix in a data-driven way. We then extracted the consensus – group representative community by applying the related community detection algorithms across the graph construction schemes (Newman,2006). See Figure 3.E for an example of a consensus matrix.

2.3.9 Agreement of consensus representative community with individual community structures

An important criterion of our analysis is the high similarity between the consensus clustering and individual clustering for every graph construction scheme that showed high group-averaged community similarity (NMI > 0.9). For that reason, we estimated this community similarity for every case.

Figure 3 illustrates the various steps of the analytic pathway.

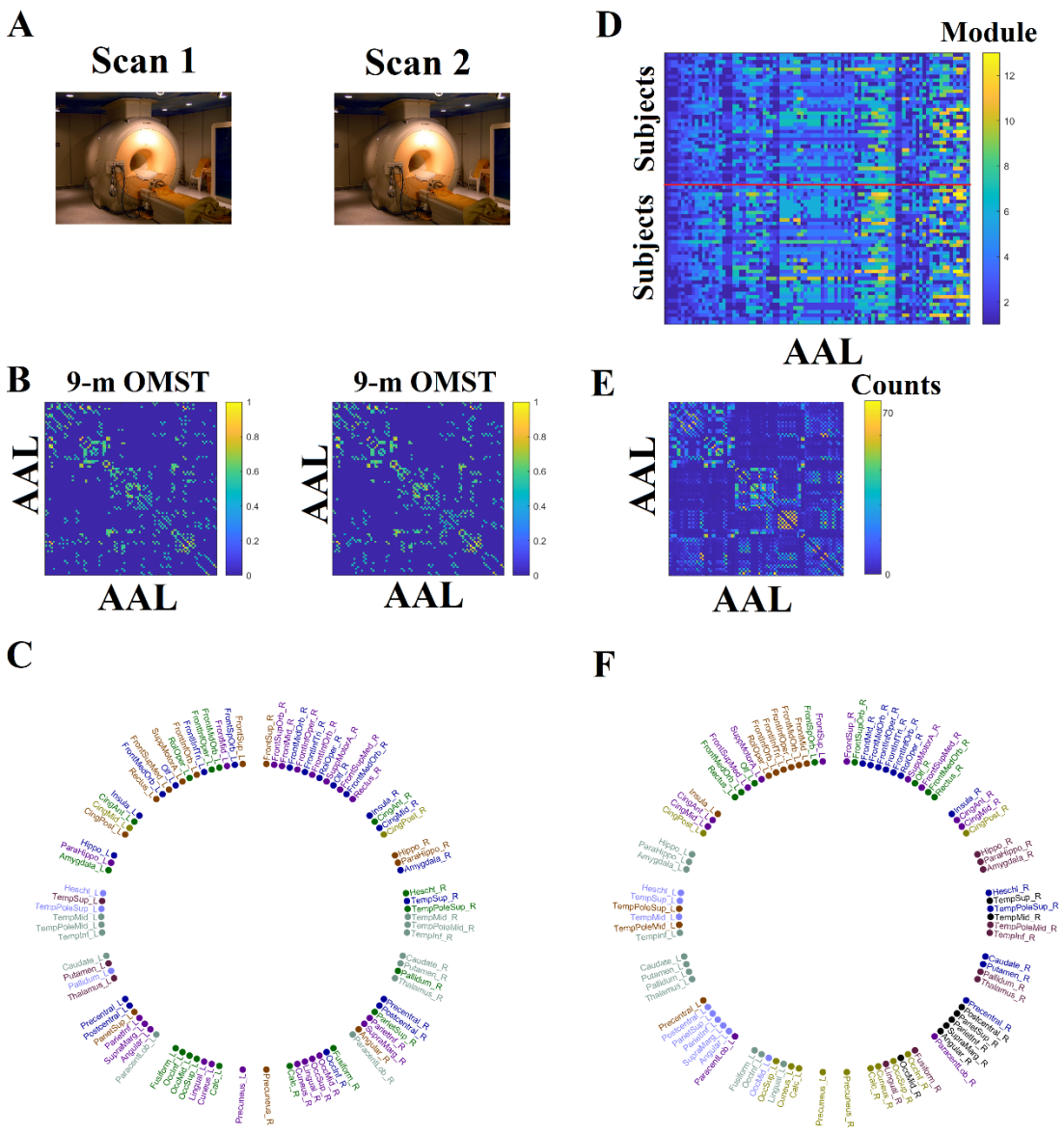

Figure 3. Outline of the presented methodology.

The demonstration based on 9-m OMST graph-construction scheme and gso-discrete mode community detection algorithm.

A. Repeat – Scan Sessions

B. Structural brain networks from subject 1 from both sessions using 9-m OMST graph-construction scheme

C. Individual community affiliation of subject 1 from scan session 1.

D. Vectorised community affiliations of the whole cohort from scan sessions 1 and 2 separated with a red line. Every module is coded with a different colour.

E. Consensus matrix is built over group community affiliations across both sessions as presented in D. Weights in the consensus matrix refer to the total number of times two

brain areas are grouped together across the cohort and scan sessions with the maximum value being (number of subjects) x (scan sessions) = 74.

F. Representative community affiliation after graph partitioning the consensus matrix presented in E. Each community is encoded to a different colour.

   Similarity NMI distance has been estimated between representative community affiliation presented in F and individual community affiliations presented in C.

2.3.10 Evaluating the Graph Construction Schemes in Combination with Community Detection Algorithms

As mentioned previously, we first selected the best combinations of graph construction schemes and community detection algorithms based on higher group-averaged between-scan community affiliation agreement (NMI > 0.9). At the second level, we adopted a criterion of highest community similarity between the consensus clustering with individual community affiliation (clustering). It is important that consensus clustering expresses the inter-subject variability and acts as a vector median for the whole group (Dimitriadis et al., 2012). Finally, the final ranking of pairs of graph construction schemes and community detection algorithms will be based on: 1) high between-scan group-averaged community similarity; and 2) high community similarity between consensus clustering and individual community affiliations (clusterings).

2.4 Modular Driven Structural Brain Hub Detection

Cognitive functions demand the integration of distributed neural activity. Complex network analysis of multimodal structural and functional brain connectivity has identified a subset of brain areas that play a key role for an efficient neural signalling and communication (van den Heuvel and Sporns, 2013). These brain areas, called hubs, support dynamic functional coupling within and between functional subnetworks. In empirical structural brain networks, the 'rich-club' term characterises brain areas/nodes with high degree that are more densely interconnected between each other compared to the rest of the network. These brain areas have a high degree meaning that they are connected with many brain areas, acting as hubs. Community partition of an SBN identifies subsets of nodes (modules) that show a relatively high level of within-module connectivity and a relatively low level of inter-module connectivity. Brain hubs can be classified into provincial and connector hubs (Guimera and Amaral, 2005) by recovering community partition at first and then estimated two modular

network metrics called participation index and within-module z-score (for further details see Appendix).

2.5 Reliability of Nodal Participation Coefficient P_i and Within-Module Z-Score z_i,

We also explored the intra-class correlation coefficient (ICC) of nodal participation coefficient P_i and within-module z-score z_i, two network metrics that have been used in brain network analysis for the detection of provincial and connector hubs. As a main outcome of this hub detection approach, we quantified the consistency of connector/provincial hub detection first within subject between scans, and secondly across the cohort.

2.6 Assessing a Reproducible Structural Core of Human Brain

We detected structural hubs for every subject, scan session and graph construction scheme by applying an absolute threshold to the participation coefficient and within-module z-score (Guimera and Amaral,2005 ; Hagmann et al., 2007,2008); van den Heuvel and Sporns,2013). We estimated an agreement index that quantifies the percentage of connector/provincial hubs that are detected in both scans. This agreement index is defined as:

$$Agreement = \sum_{k=1}^{no\ of\ subjects} \frac{CH_1 \cap CH_2}{no\ of\ subjects} \quad (4)$$

where $CH_{1,2}$ are two vectors of size 1x90 with 1s in positions where a brain area is detected as connector or provincial hub. This agreement index is normalized by the maximum number of subjects and takes the absolute value of 1 when a node/ROI is detected as either connector or provincial hub across subjects and in both scans.

3. Results

3.1 Quality of the Detected Communities

Q original values were transformed into p-values by comparing them with the 1000 surrogate (permuted) Q values. P-values ranged between 0.013 and 0.021 across subjects, scans and graph construction schemes. For soft clustering algorithms 29-32 that do not include a Q quality index, we measured the NMI between the original community affiliation and the 1000 surrogate based communities. NMI values were below 0.1 across subjects for each of the four soft clustering algorithms. This statistically significant finding allows us to include all the

subjects, scans, graph construction schemes and community detection algorithms in our overall extensive exploratory analysis.

3.2 Group-Averaged Between-Scan Agreement of Communities Affiliations

Figure 4 demonstrates group-averaged between-scan agreement of community affiliations across graph constructions schemes and community detection schemes. Based on the highest group-averaged NMI values, we detected the following four community detection algorithms across the seven graph construction schemes:

1. gso in continuous mode
2. rgso in discrete mode
3. rgso in continuous mode
4. gso in discrete mode

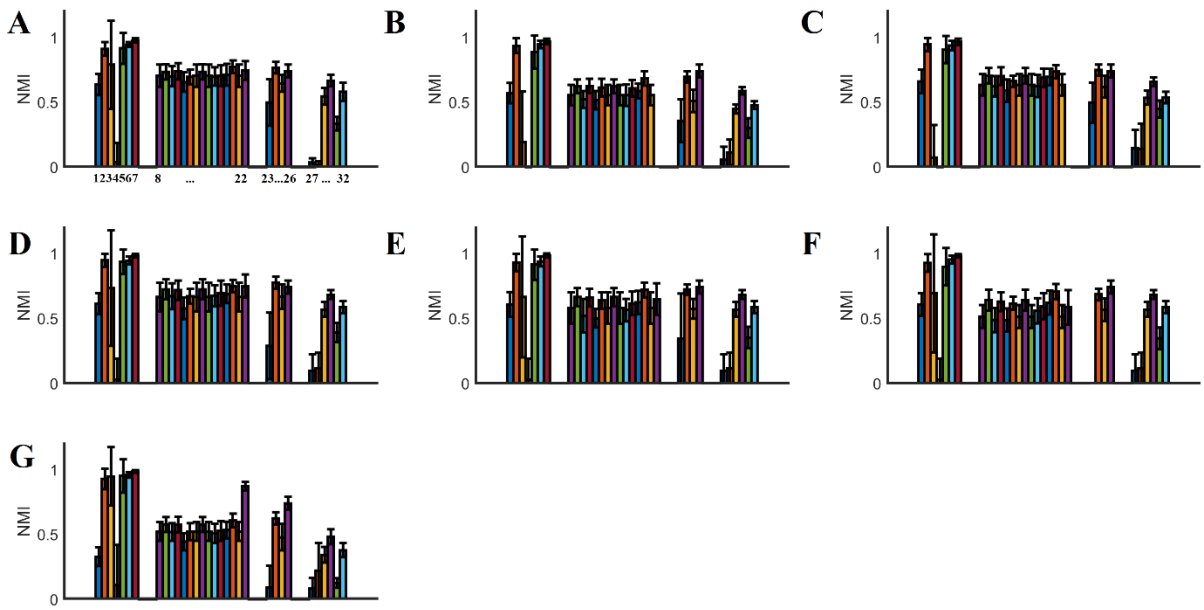

Figure 4. Between-Scan Agreement of Communities Affiliations across graph construction schemes and community detection algorithms.

Every subplot refers to one of the adopted graph-construction schemes while bars define the group-averaged between-scan agreement of community affiliations. Numbers below barplots in A. refer to the number list of community detection algorithms represented in section 2.3.3.

Community detection algorithms with the highest agreement between the two scans (NM1 > 0.9) were :gso in continuous mode, rgso in discrete mode ,rgso in continuous mode and gso in discrete mode.

A. NS-OMST

B. NS+FA OMST

C. 9-m OMST

D. NS-thr

E. NS-t/FA-w

F. NS-t/MD-w

G. FA-t/NS-w

3.3 Similarity of Individual Community Partitions with Consensus Community Partition

The highest similarity between individual community partitions and consensus community partition was detected for the combination of 9-m-OMST graph construction scheme and gso-discrete mode community detection algorithm. The second highest similarity was detected for gso-continuous mode and 9-m OMST. Rgso community detection algorithm in both continuous and discrete modes failed to produce an acceptable community similarity between a group representative community estimated via consensus clustering and the individual community affiliations (see Table 3).

Table 3. Group-averaged similarity of individual community partitions with consensus community partition. Similarities are expressed in NMI scale. We assigned with bold the top ranked values.

	NS-OMST	NS+FA OMST	9-m OMST	NS-thr	NS-t/FA-w	NS-t/MD-w	FA-t/NS-w
gso – continuous mode	0.64	0.57	**0.70**	0.61	0.61	0.61	0.39
rgso-discrete mode	0.53	0.39	0.39	0.32	0.31	0.30	0.18
rgso-continuous mode	0	0	0	0	0	0	0
gso-discrete mode	**0.69**	0.65	**0.75**	**0.68**	**0.68**	**0.68**	0.64

3.4 Evaluation of the Best Combination of Graph Construction Scheme and Community Detection Algorithm

Based on the adopted evaluation criteria for the final ranking of the pairs of graph construction schemes and community detection algorithms, and taking into account the individual scores, we ranked as the best pair the combination of gso-discrete mode with 9-m OMST. gso-discrete mode in combination with the following graph construction schemes NS-thr, NS-t/FA-w and NS-t/MD-w also gave acceptable results.

Figure 5 illustrates the topology of the nine communities across the 90 AAL brain areas based on the combination of gso-discrete mode with 9-m OMST. Importantly, modules number 1, 7 and 9 group together brain areas located within the left hemisphere, modules number 2, 6 and 8 group together brain areas located within the right hemisphere, while modules 3 – 5 involve areas from both hemispheres. Specifically, they involve bilateral ROIs from the fronto-parietal, cingulo-opercular and default mode networks like rectus, anterior and middle gyrus, frontal superior gyrus, frontal superior medial gyrus, supplementary motor area, precuneus, cuneus, calcarine and occipital superior gyrus. The bilateral superior temporal gyrus, superior temporal pole and middle temporal pole play an inter-hemispheric modular connector role (see * in Figure 5). Five out of thirteen consistent connector hubs are located within inter-hemispheric modules. Interestingly, eight homologous brain areas are grouped together in either left (module 8) or right hemisphere (module 9). These areas are: hippocampus, parahippocampal gyrus, amygdala, inferior temporal gyrus, thalamus, pallidum, fusiform and lingual gyrus.

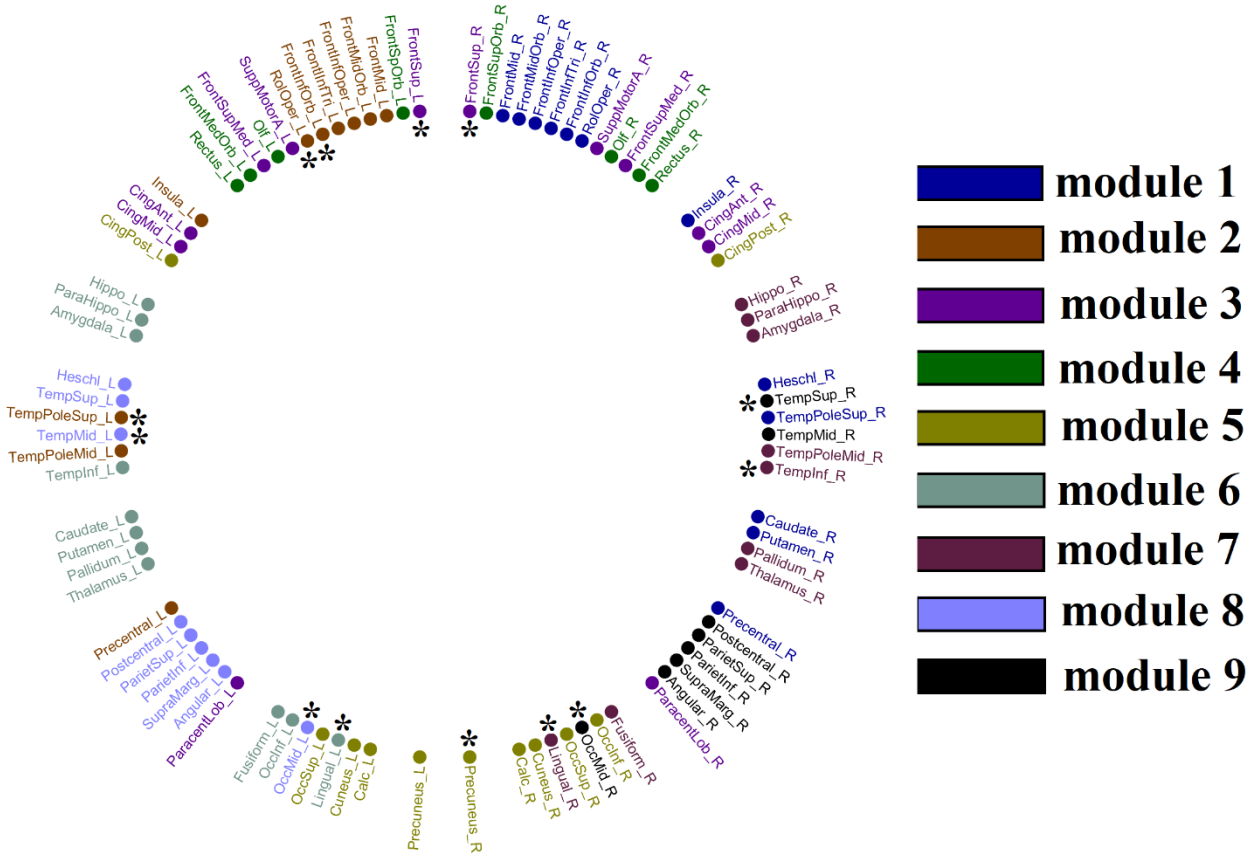

Figure 5. Topological Layout of Modular Assignment into the 90 AAL brain areas based on the community affiliation extracting from the consensus matrix related to 9-m OMST graph construction scheme and gso-discrete community detection algorithm.
With '*', we denoted the connector hubs detected consistently across subjects and repeat scans from the same combination of {9-m OMST, gso-discrete mode} (see section 3.5).
This circular plot illustrates the 90 AAL brain areas into 45 of the left hemisphere on the left semi-circle and 45 of the right hemisphere on the right semi-circle. Our analysis gave nine communities/modules where each one is encoded with a different colour.

3.5 ICC of Nodal Participation Coefficient Index and Within-Module Z-score

Table 4 shows the group-averaged ICC of nodal Participation Coefficient index P_i. ICC values were first estimated per node and then were averaged across the 90 nodes for every pair of graph construction scheme and community detection algorithms. The highest score has been detected for gso-discrete mode algorithm and for both the 9-m OMST and NS-thr graph construction schemes. On average across the seven graph construction schemes, the gso-discrete mode algorithm demonstrated the highest average ICC score. Figure 6 shows the nodal

ICC for the aforementioned pairs. Applying a Wilcoxon Rank-Sum-test between the two sets of 90 ICCs, we detected a significant difference between the two pairs (p-value = 0.041) favouring the 9-m OMST scheme.

Table 4. ICC of Nodal Participation Coefficient index across every combination of graph construction schemes with community detection algorithms. We denote the top ranked values in bold letters.

	NS-OMST	NS+FA OMST	9-m OMST	NS-thr	NS-t/FA-w	NS-t/MD-w	FA-t/NS-w
gso – continuous mode	0.54	0.50	0.62	0.67	0.58	0.60	0.38
rgso-discrete mode	0.61	0.55	0.68	0.73	0.67	0.65	0.46
rgso-continuous mode	0.58	0.55	0.68	0.67	0.61	0.61	0.43
gso-discrete mode	0.69	0.70	**0.80**	**0.80**	**0.77**	**0.76**	0.43

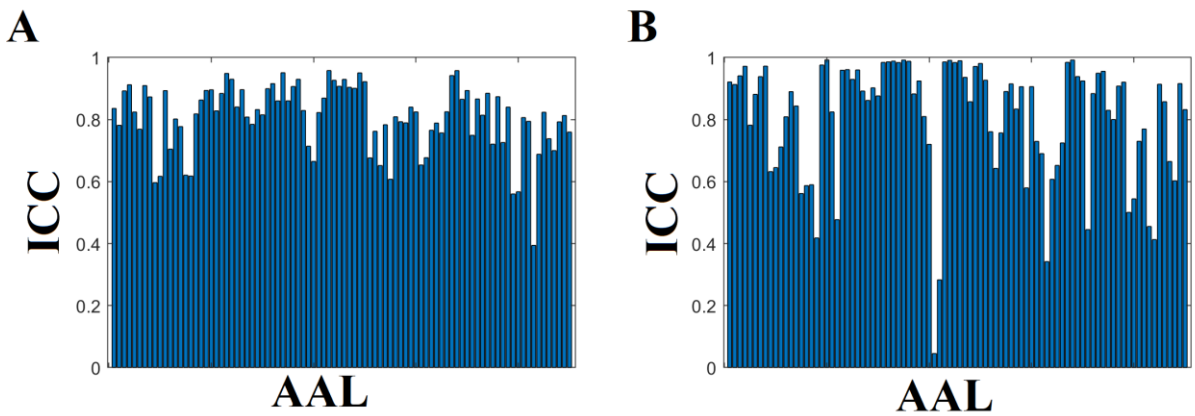

Figure 6. ICC of Nodal Participation Coefficient index for the best combinations of graph construction scheme and community detection algorithm

A. gso-discrete mode – 9-m OMST

B. gso-discrete mode – NS-thr

Table 5 shows the group-averaged ICC of nodal within-module Z-score z_i . ICC values were first estimated per node and then were averaged across the 90 brain areas for every pair of graph construction scheme and community detection algorithms. The highest scores have been detected for gso-discrete mode and rgso-discrete mode algorithms for NS-thr graph

construction scheme. On average across the seven graph construction schemes, the rgso-discrete mode algorithm demonstrated the highest average ICC score. Figure 7 demonstrates the nodal ICC for the aforementioned pairs. Applying a Wilcoxon Rank-Sum-test between the two sets of 90 ICCs, we detected a significant difference between the two pairs (p-value = 0.0335×10^{-9}) favouring the gso-discrete mode algorithm.

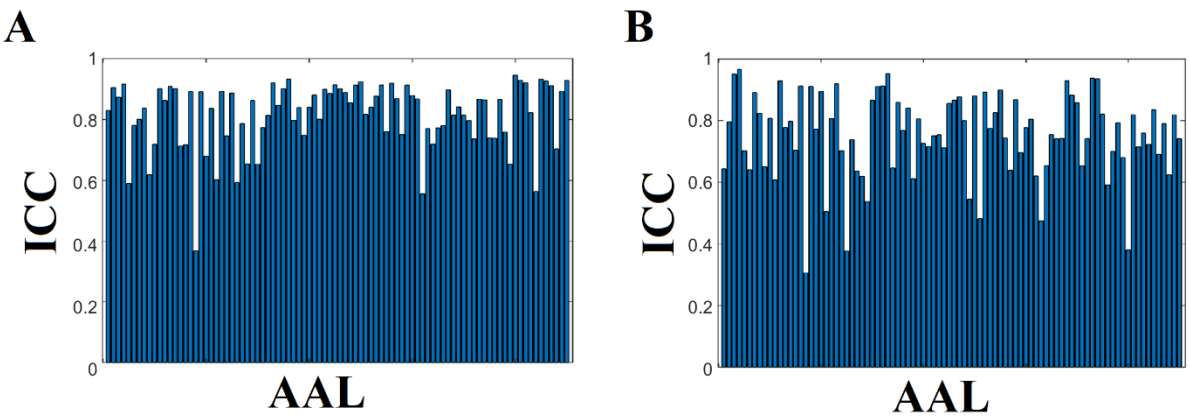

Figure 7. ICC of Nodal Within-Module Z-score for the best combinations of graph construction scheme and community detection algorithm

A. gso-discrete mode – NS-thr

B. rgso-discrete mode – NS-thr

Table 5. ICC of Nodal Within-Module Z-score across every combination of graph construction schemes with community detection algorithms. We denote the top ranked values in bold letters.

	NS-OMST	NS+FA OMST	9-m OMST	NS-thr	NS-t/FA-w	NS-t/MD-w	FA-t/NS-w
gso – continuous mode	0.71	0.66	0.65	0.79	0.69	0.69	0.69
rgso-discrete mode	**0.74**	0.66	0.64	**0.81**	0.72	0.72	0.73
rgso-continuous mode	0.56	0.57	0.60	0.68	0.55	0.57	0.61
gso-discrete mode	0.73	0.59	0.73	**0.75**	0.60	0.62	0.52

3.5 Reproducibility of Structural Hubs Detection based on Participation Coefficient Index and Within-Module Z-score

We estimated the Agreement Score of both connector and provincial hub detection across the cohort. The Agreement Score of connector hub detection across the cohort was higher than the agreement score for provincial hubs (Table 6 versus Table 7). The highest Agreement Score for connector hubs detection was found for {9-m OMST, gso-discrete mode}. Figure 8 illustrates the Agreement Score of connector hubs for this pair of algorithms. The group of connector hubs is illustrated alongside modular representation in Figure 5 and also in Table 8. Interestingly, five out of thirteen consistent connector hubs are located within the inter-hemispheric modules (see Figure 5). Our conclusion is that the combination of modular network metrics P_i and z_i succeeded in uncovering a consistent core of connector hubs but it failed to detect provincial hubs consistently.

Table 6. Agreement Scores of Provincial Hubs across every combination of graph construction scheme and community detection algorithm. We assigned with bold the top ranked values.

	NS-OMST	NS+FA OMST	9-m OMST	NS-thr	NS-t/FA-w	NS-t/MD-w	FA-t/NS-w
gso – continuous mode	0.69	**0.72**	0.75	0.60	0.58	0.517	0.52
rgso-discrete mode	0.46	0.29	0.28	0.30	0.31	0.30	0.21
rgso-continuous mode	0.00	0.00	0.27	0.00	0.00	0.00	0.00
gso-discrete mode	0.69	0.73	**0.83**	**0.80**	0.59	0.61	0.24

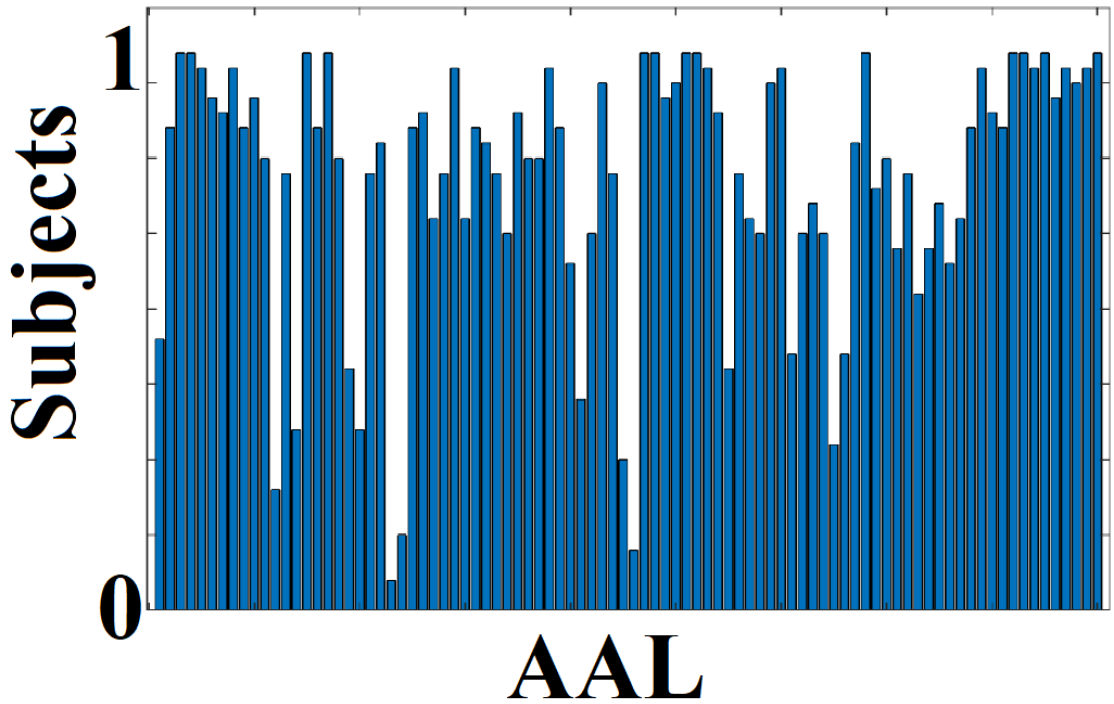

Figure 8. Agreement Score of Connector Hubs for the best pair of {9-m OMST, gso-discrete mode}.

Table 7. Agreement Scores of Connector Hubs across every combination of graph construction scheme and community detection algorithm. We assigned with bold the top ranked values.

	NS-OMST	NS+FA OMST	9-m OMST	NS-thr	NS-t/FA-w	NS-t/MD-w	FA-t/NS-w
gso – continuous mode	0.40	0.13	0.23	0.38	0.32	0.31	0.43
rgso-discrete mode	**0.65**	0.42	0.45	**0.67**	0.57	0.58	**0.80**
rgso-continuous mode	0.13	0.05	0.09	0.19	0.15	0.14	0.49
gso-discrete mode	0.17	0.03	0.05	0.12	0.12	0.12	0.17

Table 8. List of consistent connector hubs aligned with the detected modular number illustrated topologically in Figure 5.

Connector Hubs	Module Number
FrontSup_L	3
FrontSup_R	3
FrontInfOrb_L	2
RolOper_L	2
Lingual_L	6
Lingual_R	7
OccMid_L	8
OccMid_R	9
Precuneus_R	5
TempSup_R	9
TempPoleSup_L	2
TempMid_L	8
TempInf_R	7

4. Discussion

We have presented the first extensive study in the literature on the robustness of community detection in structural brain networks by exploring different graph-construction schemes and various community detection algorithms. The analysis was performed in a test-retest dataset from the Human Connectome Project. Our main findings have direct implications for longitudinal studies and in studies comparing healthy controls versus diseased populations.

The key findings of our analysis can be summarized as follows:

1. The reproducibility of community affiliations depends heavily on the combination of graph-construction scheme and community detection algorithm. All previously reported studies of network communities adopted a main graph-construction scheme and community detection algorithm, with the majority of them focused on Newman's modularity objective criterion (Newman, 2006; Sporns and Betzel, 2016; Betzel et al., 2017). Based on our first criterion of high reproducibility of community affiliation

between the two scans and across the cohort (NMI > 0.9), we revealed four community detection algorithms as the best choices:

A. gso in continuous mode
B. rgso in discrete mode
C. rgso in continuous mode
D. gso in discrete mode

These four algorithms gave excellent reproducibility across the entire set of graph-construction schemes (see Table 2 and Figure 4).

2. Our second criterion was the high similarity of consensus community affiliation with individual community affiliations. The majority of the neuroimaging studies that employed a single graph-construction scheme and one community detection algorithm did not evaluate their findings under this framework (Ryali et al., 2015 ; Rosero et al., 2017; Akiki and Abdallah, 2019). The consensus matrix integrates community affiliations across the entire cohort counting the number of times two nodes (ROIs) are assigned to the same community. To reveal a representative community affiliation, we have to apply a community detection algorithm. However, almost all previous studies report this representative community affiliation without estimating its similarity with *individual* community affiliations. Here, we found the highest similarity between individual community partitions and representative community partition for the 9-m-OMST graph construction scheme and gso-discrete mode community detection algorithm. In general, the rgso community detection algorithm in both continuous and discrete modes failed to produce an acceptable representative community partition (see Table 3). The second highest similarity was detected for gso-continuous mode and 9-m OMST.
3. An important result of our analysis is that soft clustering community detection algorithms gave the least reproducible results. Therefore, we recommend the use of hard-clustering algorithms for the detection of brain communities, at least when using the AAL template.
4. The best combination of graph-construction scheme (9-m OMST) and community detection algorithm (gso-discrete mode) revealed nine distinct modules as illustrated topologically in Figure 5. The topology of these modules uncovered interesting findings:

A. Modular numbers 1, 7 and 9 group together brain areas located exclusively within the left hemisphere while module number 2, 6 and 8 group together brain areas

located exclusively within the right hemisphere. Module 3 – 5 group brain areas from both hemispheres together.

B. Modules 3 – 5 that integrate brain areas from both hemispheres involve bilateral ROIs from fronto-parietal, cingulo-opercular and default mode network like rectus, anterior and middle gyrus, frontal superior gyrus, frontal superior medial gyrus, supplementary motor area, precuneus, cuneus, calcarine and occipital superior gyrus. A multi-tasking fMRI study has previously suggested the flexible role of the fronto-parietal network in cognitive control and adaptive demands of cognitive tasks (Cole et al., 2013).

C. Five out of thirteen consistent connector hubs are located within inter-hemispheric modules 3 – 5 supporting their inter-connecting role (Figure 5).

D. Interestingly, eight homologous brain areas were grouped together in either left (module 8) or right hemisphere (module 9). These areas are: hippocampus, parahippocampal gyrus, amygdala, inferior temporal gyrus, thalamus, pallidum, fusiform and lingual. Lesions of hippocampus, parahippocampal gyrus, amygdala and fusiform gyrus in subjects with temporal lobe epilepsy caused an impaired associative memory in learning tasks that require learning and recall of objects and faces (Weniger et al., 2004). These four brain areas including the thalamus are the brain areas most consistently implicated in neurodegenerative dementias, especially in Alzheimer's Disease, even at an early stage (Manuello et al., 2018).

E. Bilateral superior temporal gyrus, superior temporal pole and middle temporal pole play an inter-hemispheric modular integrated role. Inter-hemispheric functional connections between temporal lobes predict language impairment in adolescents born preterm (Northam et al., 2012). Phonological awareness, a key factor in reading acquisition was positively correlated with radial diffusivity of the interhemispheric pathways connecting temporal lobes (Dougherty et al. 2007). This bilateral temporal module could play a key role in many functions and dysfunctions.

5. The core of our study was to carry out an extensive analysis of the best choice of the pair graph-construction scheme and community detection algorithm. As a consequence of this choice, connector and provincial hubs detection based upon two modular network metrics called participation coefficient score P_i and within-module z-score z_i will be also affected. Our results revealed a high reproducibility of nodal P_i in the gso-discrete mode algorithm and for both 9-m OMST and NS-thr graph construction schemes favouring 9-m OMST and a high reliability of nodal z_i for both gso-discrete

mode and rgso-discrete mode algorithms with NS-thr graph construction scheme favouring gso-discrete mode algorithm.

6. However, the Agreement Score was high only for connector and not for provincial hubs using both modular network metrics. We detected a group of thirteen reproducible connector hubs across the cohort. Based on our results, we therefore recommend to not use these modular network metrics for the detection of provincial hubs, at least when using the AAL atlas. The designation of a brain node as a hub depends also on the scale at which brain networks are constructed. Many brain areas in a basic atlas template group together functionally heterogenous subareas and it is possible that a finer-grained parcellation may affect the nodes' classification as a hub or not. For example, the thalamus, despite comprising 50 – 60 specialized sub-nuclei (Herrero et al., 2002) is in many studies, including ours, treated as a single node.

In our previous study on the same cohort, we focused on the reproducibility of network topologies focusing on edge weights and graph theoretical metrics. We demonstrated that network topology and edge weights are reproducible but the reproducibility depends on the graph-construction scheme (Messaritaki et al., 2019). As shown here, the reproducibility of network topologies and edge weights does not guarantee the reproducibility of community detection at the mesoscale. In the present study, we focused on this important tool for mesoscale network topological investigations, the detection of robust communities in structural brain networks over a set of subjects following a repeat scan protocol. This is the first study in the literature that explores the robustness of community detection over a large set of graph-construction schemes (seven) and community detection algorithms (thirty-two). Our analysis detected an optimal pair of {9-m OMST, gso-discrete mode} that supports the two basic criteria reported as significant for acceptable results: the first is the high reproducibility of communities affiliations between the two scan-sessions and the second is the high similarity of representative community affiliations with the individual community affiliations. To the best of our knowledge, this is the first time that the second criterion was used for the validation of representative consensus community affiliation even in the case of using a single graph-construction scheme and community detection algorithm.

Our study has a few limitations due to the nature of the HCP dataset. This dataset involves a specific data acquisition protocol and also different tractography algorithms. We recommend to follow our analysis for every study because such an investigation could increase the reproducibility of the findings at the mesoscale while also increasing the power of the study at

the nodal and network level (Messaritaki et al., 2019). Three or more scan sessions would be also desirable to get a more robust assessment of reproducibility. Lastly, the reproducibility of structural brain networks is affected by the resolution of the MR data (Vaessen et al., 2010), the parcellation scheme used (Bassett et al., 2011), the interval time between the scan sessions and others. These variables should also be considered in structural brain networks following our data-driven analysis. However, here we focused on how the reliability of community detection in structural brain networks is affected by two important variables: the graph-construction scheme and community detection algorithm (Welton et al., 2015).

5. Conclusions

In this study, we compared several graph-construction schemes and community detection algorithms for the detection of reproducible communities in structural brain networks. Our extensive analysis showed that every choice in both groups of algorithms exhibits different reproducibility in community detection algorithms and also in connector/provincial hubs detection. Our analysis indicates that our analytic pathway should be adopted and performed in every study in order to extract reliable results at the mesoscale of structural brain networks.

Declarations of interest

None.

Author Contributions

Conceptualization: SID

Methodology:SID

Software:SID

Validation:SID

Formal analysis:SID

Formal Analysis: SID

Investigation:SID

Resources: The original diffusion MRI are free available from the Human Connectome project. The analysis of tractography and the construction of structural brain networks has been realized by EM.

Data curation:EM,SID

Roles/Writing - original draft: SID,

Writing - review & editing: EM,DJ

Funding acquisition:EM,SID

Data and code availability

The HCP test-retest data is freely available as listed above. The code used to generate the graphs for the structural brain networks with the OMST schemes is available at: h*ttps://github.com/stdimitr/multi-group-analysis-OMST-GDD*. The structural brain networks and the code used to perform the reproducibility analysis will be released as soon as the paper will be accepted from author's github website https://github.com/stdimitr.
Source code of community detection algorithms are provided on the Dr.Le Martelot's personal homepage, author's homepage and also were implemented by our team. The collection of the whole set of the algorithms will be reported in our github homepage.

Acknowledgements

We are grateful to the Human Connectome Project for making the test-retest data freely available. The work was partly funded under the BRAIN Biomedical Research Unit, which is funded by the Welsh Government through Health and Care Research Wales. DKJ is supported by a Wellcome Trust Investigator Award (096646/Z/11/Z) and a Wellcome Trust Strategic Award (104943/Z/14/Z). SID was supported by MRC grant MR/K004360/1 and a Marie Sklodowska-Curie COFUND EU-UK Research Fellowship. EM is supported by a Wellcome Trust ISSF Research Fellowship at Cardiff University (204824/Z/16/Z).

References

Aerts H, W. Fias, K. Caeyenberghs, D.,2016. MarinazzoBrain networks under attack: robustness properties and the impact of lesions Brain, 139, 3063-3083

Ahn YY , Bagrow JP , Lehmann S.,2010. Link communities reveal multiscale complexity in networks. Nature 466, 761–764

Akiki, TJ, Abdallah, CG.,2019. Determining the hierarchical architecture of the human brain using subject-level clustering of functional networks. Scientific Reports volume 9, Article number: 19290

Arenas, A., Fernandez, A., and Gomez, S., 2008. Analysis of the structure of complex networks at different resolution levels. New Journal of Physics, 10, 053039.

Avena-Koenigsberger, A., Misic, B. & Sporns, O.,2017. Communication dynamics in complex brain networks. Nat. Rev. Neurosci. 19, 17–33

Baker,S.T.E., Lubman, D.I., Yucel,M., Allen, N.B. , Whittle, S., Fulcher, B.D., Zalesky, A., Fornito, A.,2015. Developmental changes in brain network hub connectivity in late adolescence.J. Neurosci., 35 (24), 9078-9087

Bassett, D.S., Wymbs, N.F., Porter, M.A., Mucha, P.J., Carlson, J.M., Grafton, S.T., 2011. Dy1297 namic reconfiguration of human brain networks during learning. Proc. Natl. Acad. 1298 Sci. U. S. A. 108, 7641–7646.

Bassett, D.S., Brown, J.A., Deshpande, V., Carlson, J.M., Grafton, S.T., 2011. Conserved and variable architecture of human white matter connectivity. Neuroimage 54:1262–1279

Bassett, D. S. & Sporns, O.,2017. Network neuroscience. Nat. Neurosci. 20, 353–364

Bassett, D.S. & Mattar M.G.,2017.A Network Neuroscience of Human Learning: Potential To Inform Quantitative Theories of Brain and Behavior.Trends Cogn Sci. 21(4), 250–264.

Betzel, R.F., Medaglia, J.D., Papadopoulos, L., Baum, G., Gur, R., Gur, R., Roalf, D., Satterthwaite, T.D., Bassett, D.S., 2017. The modular organization of human anatomical brain networks: Accounting for the cost of wiring. Network Neuroscience, 1(1), 42–68

Blondel, Vincent D; Guillaume, Jean-Loup; Lambiotte, Renaud; Lefebvre, Etienne (9 October 2008). "Fast unfolding of communities in large networks". Journal of Statistical Mechanics: Theory and Experiment. 2008 (10): P10008

Borgatti, S.P., Everett, M.G.,2000.Models of core/periphery structures

Social. Netw., 21 (4),375-395

Braun, U., Schäfer, A., Walter, H., Erk, S., Romanczuk-Seiferth, N., Haddad, L., Schweiger, J.I., 610 Grimm, O., Heinz, A., Tost, H., Meyer-Lindenberg, A., Bassett, D.S., 2015. Dynamic 611 reconfiguration of frontal brain networks during executive cognition in humans. Proc. Natl. 612 Acad. Sci. U.S.A. 112, 11678–83.

Braun,U., Schäfer,A., Bassett,D.S., Rausch,F., Schweiger, J.I., Bilek,E., Erk,S., Romanczuk Seiferth,N., Grimm, O., Geiger,L.S., Haddad,L., Otto,K., Mohnke, S., Heinz, A., Zink, M., Walter, H., Schwarz, E. , Meyer-Lindenberg, A., Tost, H. , 2016.Dynamic brain network reconfiguration as a potential schizophrenia genetic risk mechanism modulated by NMDA receptor function . Proc. Natl. Acad. Sci. USA, 113 (44), 12568-12573

Cole M.W., Reynolds J.R., Power J.D., Repovs G., Anticevic A., Braver T.S.Multi-task connectivity reveals flexible hubs for adaptive task control.Nat. Neurosci., 16 (9) (2013), pp. 1348-1355,

Colizza V, A. Flammini, M.A. Serrano, A.,2006. Vespignani. Detecting rich-club ordering in complex networks.Nat. Phys., 2 (2), 110-115

Collin G, M.P. van den Heuvel, L. Abramovic, A. Vreeker, M.A. de Reus, N.E. M van Haren, M.P.M. Boks, R.A. Ophoff, R.S.,2016. KahnBrain network analysis reveals affected connectome structure in bipolar disorder Hum. Brain Mapp., 27,122-134

Danon, L., D´ıaz-Guilera, A., Arenas.A.,2006. The effect of size heterogeneity on community identification in complex networks. Journal of Statistical Mechanics: Theory and Experiment, (11),P11010

Dimitriadis, S. I., Laskaris, N. A., Del Rio-Portilla, Y., and Koudounis, G. C. (2009). Characterizing dynamic functional connectivity across sleep stages from EEG. Brain Topogr. 22, 119–133.

Dimitriadis, S. I., Kanatsouli, K., Laskaris, N. A., Tsirka, V., Vourkas, M., and Micheloyannis, S. (2012). Surface EEG shows that Functional Segregation via phase coupling contributes to the neural substrate of mental calculations. Brain Cogn. 80, 45–52.

Dimitriadis,S.I., Antonakakis,M., Simos,P., Fletcher,J.M., A.C. Papanicolaou,A. C.,2017a.Data-driven Topological Filtering Based on Orthogonal Minimal Spanning Trees: Application to Multi-Group MEG Resting-State Connectivity.Brain Connectivity 7(10),661-670.

Dimitriadis,S.I., Drakesmith,M., Bells,S., Parker,G.D., Linden,D.E., D.K. Jones, D.K.,2017b.Improving the reliability of network metrics in structural brain networks by integrating different network weighting strategies into a single graph.Front. Neurosci., 11, p. 694

Dimitriadis, S.I., Salis,C., Tarnanas,I., Linden,D.E.,2017c.Topological filtering of dynamic functional brain networks unfolds informative chronnectomics: a novel data-driven thresholding scheme based on orthogonal minimal spanning trees (OMSTs).Front. Neuroinf., 28,p.11

Dong, X., Frossard, P., Vandergheynst, P., Nefedov, N., 2014. Clustering on multi-layer graphs via subspace analysis on grassmann manifolds. Signal Processing, IEEE Transactions on 62(4),905–918

Dougherty, R. F., Ben-Shachar, M., Deutsch, D. K., Hernandez, A., Fox, G. R., and Wandell, B. A., 2007. Temporal-callosal pathway diffusivity predicts phonological skills in children. Proc. Natl. Acad. Sci. U.S.A. 104, 8556–8561

Drakesmith,M, K. Caeyenberghs, A. Dutt, S. Zammit, C.J. Evans, A. Reichenberg, G. Lewis, A.S. Dvid, D.K. Jones,2015.Schizophrenia-like topological changes in the structural connectome of individuals with subclinial psychotic experiences
Hum. Brain Mapp., 36, 2629-2643

Fortunato, S., 2010. Community detection in graphs. Phys Rep 486,(3-5),75–174

Fortunato, S., Castellano, C., 2012. Community structure in graphs Computational Complexity. Springer, 490–512.

Friston, K.J., 2011. Functional and effective connectivity: a review. Brain Connect 1(1),13–36.

Giusti, G., Ghrist,R., Bassett,D.S.,2016.Two's company, three (or more) is a simplex: algebraic-topological tools for understanding higher-order structure in neural data.J. Comput. Neurosci., 41(1),1-14

Guimera, R. and Amaral, L.A.N., 2005. Functional cartography of complex metabolic networks. Nature 433, 895–900

Hagmann, P., Kurant, M., Gigandet, X., Thiran, P., Wedeen, V.J., et al., 2007. Mapping human whole-brain structural networks with diffusion MRI. PLoS One 2, e597

Herrero, M.T., Barcia,C., Navarro.,J.M.,2002.Functional anatomy of thalamus and basal ganglia.Child’s Nerv. Syst., 18,386-404

Huang, J., Sun, H., Liu, Y., Song, Q., and Weninger, T., 2011. Towards online multiresolution community detection in large-scale networks. PLoS ONE, 6, e23829.

Kernighan, B. W.; Lin, Shen,1970. An efficient heuristic procedure for partitioning graphs". Bell System Technical Journal. 49: 291–307

Imms,P., Clemente,A., Cook,M., D'Souza,W., Wilson,P.H., Jones,D.K., Caeyenberghs,K.,2019.The structural connectome in traumatic brain injury: a meta-analysis of graph metrics Neuroscience and Behavioural Reviews, 99, 128-137

Lancichinetti A, Fortunato S (2009a) Community detection algorithms: a comparative analysis. Physical Review E 80(5 Pt 2):
056117.

Lancichinetti, A., Fortunato, S. Kertesz, J.,2009b. Detecting the overlapping and hierarchical community structure in complex networks. N. J. Phys. 11, 033015
Lancichinetti,A., & Fortunato,S., 2012. Consensus clustering in complex networks. Scientific Reports 2, Article number: 336.

Leemans, A., Jeurissen, B., Sijbers, J., Jones, D., 2009. ExploreDTI: a graphical toolbox for processing, analyzing, and visualizing diffusion MR data. Proceedings of the International Society for Magnetic Resonance in Medicine, Honolulu, Hawaii.

Le Martelot, E., Hankin, C.,2011. Multi-scale community detection using stability as optimisation criterion in a greedy algorithm. KDIR, 216–225.

Le Martelot E, Hankin C,2012a. Multi-scale community detection using stability optimisation. Int J Web Based Communities, 9,323–348.

Le Martelot E, Hankin C,2012b. Fast multi-scale detection of relevant communities in large-scale networks. Comput J , 56, 1136–1150.

Manuello, J., Nani, A., Premi, E., Borroni, B., Costa, T., Tatu, K.,
et al.,2018. The pathoconnectivity profile of alzheimer's disease: a morphometric coalteration network analysis. Front Neurol 8,739

Messaritaki, E., Dimitriadis,S.I., Jones,D.K.,2019a.Assessment of the reproducibility of structural brain networks derived using different edge-weighting streategies Proceedings of the 27th Annual Meeting of the ISMRM, Montreal, Canada

Messaritaki, E.,Dimitriadis,S.I., D.K. Jones.,D.K.,2019b. Optimization of graph construction can significantly increase the power of structural brain network studies. NeuroImage 199(1),495-511

Meunier, D., Lambiotte, R., Fornito, A., Karen, D.E., Bullmore, E.T.,2009. Hierarchical modularity in human brain functional networks. Frontiers in neuroinformatics,3,37

Meunier, D., Lambiotte, R., Bullmore, E.T.,2010. Modular and hierarchically modular organization of brain networks. Front Neurosci 8;4:200.

Nelson, B.G., Bassett,D.S., Camchong, J., Bullmore,E.T., Lim,K.O.,2017.Comparison of large-scale human brain function and anatomical networks in schizophrenia
Neuroimage: Clinic, 15,439-448

Newman, M.E., Girvan, M.,2004. Finding and evaluating community structure in networks. Physical Review E 69(2 Pt 2): 026113

Newman, M.E.J., 2006. Modularity and community structure in networks. Proc Natl Acad Sci U S A 103,8577–8582.

Newman, M.E.J., 2012. Communities, modules and large-scale structure in networks. Nat Phys 8(1),25–31

Northam, G.B., Liégeois, F., Tournier, J.D., et al.,2012. Interhemispheric temporal lobe connectivity predicts language impairment in adolescents born preterm. Brain,135(Pt 12),3781–3798

Pavan,M., Pellilo.,M.,2017.Dominant sets and pairwise clustering.IEEE Trans on PAMI, 29,167-172

Owen, J.P., Ziv,E., Bukshpun,P., Pojman,N., Wakahiro,M., Berman,J.I., Roberts, T.P.,Fried man,E.J., Sherr, E.H., Mukherjee,P.,2013.Test-retest reliability of computational network measurements derived from the structural connectome of the human brain.Brain Connect., 3, 160-176

Ozdemir, A., Bolanos, M., Bernat, E., Aviyente, S., 2015. Hierarchical Spectral Consensus Clustering for Group Analysis ofFunctional Brain Networks. IEEE Trans Biomed Eng 62(9),2158–2169

Palla, G., Derényi, I., Farkas, I., Vicsek,T.,2005. Uncovering the Overlapping Community Structure of Complex Networks in Nature and Society. Nature 435, 814–818

Park, H.J., Friston, K.J.,2013. Structural and Functional Brain Networks: From Connections to Cognition. Science 342(6158),1238411

Pessoa, L.,2018.Understanding emotion with brain networks. Curr Opin Behav Sci.,19,19–25.

Psorakis, I., Roberts,S., Ebden,M., Sheldon. B.,2011.Overlapping Community Detection using Nonnegative Matrix Factorization. Physical Review E 83, 066114

Radicchi, F., Castellano, C., Cecconi, F., Loreto, V., Parisi, D., 2004. Defining and identifying communities in networks. ProcNatl Acad Sci U S A 101(9),2658–2663.

Reichardt, J.,Bornholdt, S., 2006. Statistical mechanics of community detection. Physical Review E, 74, 016110.

Ronhovde, P., Nussinov, Z., 2009. Multiresolution community detection for megascale networks by information-based replica correlations. Physical Review E, 80, 016109.

Rasero, J., Pellicoro, M., Angelini, L., Cortes, J.M., Marinazzo, D., Stramaglia, S.,2017. Consensus clustering approach to group brain connectivity matrices. Netw Neurosci., 1(3),242–253

Reichardt, J., Bornholdt, S., 2006. Statistical mechanics of community detection. Phys. Rev. E 74(1):016110

Rosvall, M., Bergstrom, C.T., 2008. Maps of random walks on complex networks reveal community structure. Proc Natl Acad Sci USA 105,1118–1123.

Rubinov, M., Sporns, O., 2010. Complex network measures of brain connectivity: uses and interpretations. NeuroImage 52(3),1059–1069.

Ryali, S., Chen, T., Padmanabhan, A., Cai, W., Menon, V.,2015. Development and validation of consensus clustering-based framework for brain segmentation using resting fMRI. J Neurosci Methods. 240,128–140.

Shi, J., Malik, J.,2000. Normalized cuts and image segmentation. IEEE Trans. Pattern Anal. Mach. Intell. 22(8), 888–905

Smith, R.E., Tournier, J.D., Calamante, F., Connelly,A.,2015.The effects of SIFT on the reproducibility and biological accuracy of the structural connectome. Neuroimage, 104, 253-265

Sotiropoulos,S.N., Jbabdi,S., Xu,J., Andersson,J.L., Moeller,S., Auerbach,E.J., Glasser, M.F., Hernandez, M., Sapiro,G., Jenkinson,M., D.A. Feinberg,D.A., Yacoub,E., Lenglet,C., Essen,D.C.V., Ugurbil,K., Behrens,T.E.,2013a.Advances in diffusion MRI acquisition and processing in the human connectome project.Neuroimage, 80,125-143

SotiropoulosSN, S. Moeller, S. Jbabdi, J. Xu, J.L. Anderson, E.J. Auerbach, E. Yacoub, D. Fe inberg, K. Setsompop, L.L. Wald, T.E.J. Behrend, K. Ugurbil, C. Lenglet,2013b. Effects of image reconstruction on fibre orientation mapping from multichannel diffusion MRI: reducing the noise floor using SENSE. Magn. Reson. Med., 70 (6) (2013b), pp. 1682-1689

Sporns, O, Tononi, G, Edelman, G M. Theoretical neuroanatomy: relating anatomical and functional connectivity in graphs and cortical connection matrices. Cerebral cortex. 10(2):127–141.2000

Sporns, O., 2013. Network attributes for segregation and integration in the human brain. Curr Opin Neurobiol 23(2),162–171.

Sporns, O. & Betzel, R.F.,2016. Modular brain networks. Annu. Rev. Psychol. 67, 613–640.

TzourioMazoyer,N., Landeau,B., Papathanassiou,D., Crivello,F., Etard,O., Delcroix,N., Maz oyer,B., Joliot,M.,2002.Automated anatomical labeling of activations in SPM using a macroscopic anatomical parcelation of the MNI MRI single-subject brain. Neuroimage, 15,273-289
meso
Yuan,J.P., HenjeBlom,E., Flynn,T., Chen,Y., Ho,T.T., Connolly,C.G., DumontWalter,R.A., Yang,T.T., Xu,D.,Tymofiyeva,O.,2019.Test-retest Reliability of Graph Theoretical Metrics in Adolescent Brains. Brain Connect. 9(2),144-154

Vaessen, M.J., Hofman, P.A.M., Tijssen, H.N., Aldenkamp, A.P., Jansen, J.F.A., Backes W.H.,2010. The effect and reproducibility of different clinical DTI gradient sets on small world brain connectivity measures. NeuroImage 51,1106–1116

van den Heuvel, M.P. and Sporns, O., 2011. Rich-club organization of the human connectome. J. Neurosci. 31, 15775–15786

van den Heuvel, M. P. & Sporns, O.,2013. Network hubs in the human brain. Trends Cogn. Sci. 17, 683–696

Vidaurre, D.R., Becker,A.R., Quinn, A.J., Alfaro-Almagro, F., Smith, S.M., Woolrich, M.W., 2018.Discovering dynamic brain networks from big data in rest and task.Neuroimage, 180 (B), 646-656

Welton, T., Kent, D.A. , Auer, D.P., Dineen,R.A.,2015. Reproducibility of graph-theoretic brain network metrics: a systematic review. Brain Connect., 5 (4),193-202

Weniger, G., Boucsein, K., Irle, E.,2004.Impaired associative memory in temporal lobe epilepsy subjects after lesions of hippocampus, parahippocampal gyrus, and amygdala. Hippocampus. 14(6),785-96.

Zhong, S., He,Y., Gong.G,2015.Convergence and divergence across construction methods or human brain matter networks: an assessment based on individual differences.Hum. Brain Mapp., 36,1995-2013

Appendix 1. Detecting Structural Hubs based on Nodal Participation Coefficient P_i and Within-Module Z-Score z_i

By recovering the community partition and estimating the participation coefficient, we can classify brain hubs into provincial and connector hubs (Guimera and Amaral,2005). 'Provincial hubs' are high-degree nodes that primarily connect to nodes in the same module. 'Connector hubs' are high-degree nodes that show a diverse connectivity profile by connecting to several different modules within the network. Brain hubs are important brain areas that are vulnerable and susceptible to disconnection and dysfunction in brain disorders. Rich club organization of structural hubs supports the robustness of inter-hub connections and promotes the efficient information exchange between brain areas and its integration across the brain (van den Heuvel and Sporns,2011).

The distinction of nodes into hubs and non-hubs by a combination of network topology and community affiliation is supported by a pair of network metrics called: participation coefficient P_i and within-module z-score, z_i. This definition has been first reported by Guimera and Amaral (2005). Here, we first reported the reliability of these nodal metrics in structural brain networks.

The degree of a node i is defined as $k_i = \sum_j A_{ij}$, where A_{ij} is the adjacency matrix of the graph. Within-module z-score for node i is defined as

$$z_i = \frac{\kappa_i - \bar{\kappa}_{s_i}}{\sigma_{s_i}}, \quad (1)$$

where κ_i is the number of edges of node i to other nodes in its module s_i , $\bar{\kappa}_{s_i}$ is the average of κ over all the nodes in s_i , and σ_{si} is the standard deviation of κ in s_i .

The participation coefficient index P_i, for node i is defined as

$$P_i = 1 - \sum_{s=1}^{N_M} \left(\frac{\kappa_{is}}{\kappa_i} \right)^2 \quad (2)$$

where k_{is} is the number of links of node i to nodes in module s, and k_i is the total degree of node i. The participation coefficient of a node is therefore close to one if its links are uniformly distributed among all the modules and zero if all its links are within its own module.

Provincial Hubs: If a node with a large degree, $k \gg 1$, has at least 5/6 of its links within the module, then it follows that $P = 1 - (5/6)^2 - (k/6)(1/k^2) = 0.31 - 1/(6k) \approx 0.30$.

Connector Hubs: If a node with a large degree has at least half of its links within the module, then it follows that $P = 1 - 1/4 - (k/2)(1/k^2) = 0.75 - 1/(2k)$. Since $k \gg 1$, $P < 0.75$ for such nodes.

Both provincial and connector hubs demonstrate a high within-module z-score which means that they have many within-module edges. In this work, we used the threshold originally proposed by Guimera and Amaral,(2005) for the z_i dimension as $z_i > 2.5$ for both types of studied hubs (see Figure 5 in Guimera and Amaral,(2005)). In the P_i dimension, we defined a node as provincial hub if $P_i <= 0.3$ and as connector hub if $0.3 < P_i < 0.75$.

The intra-class correlation coefficient (ICC) was estimated for every nodal participation coefficient index, P_i, and within-module z-score z_i across the cohort and for every selected pair of graph construction schemes and community detection algorithms that showed higher group-averaged community similarity (NMI > 0.9).